



Supplement of

The real part of the refractive indices and effective densities for chemically segregated ambient aerosols in Guangzhou by a single particle aerosol mass spectrometer

G. Zhang et al.

Correspondence to: X. Bi (bixh@gig.ac.cn)

The copyright of individual parts of the supplement might differ from the CC-BY 3.0 licence.

16 **1 The meteorological conditions over the study**

17 Temporal profiles (in 1 hour resolution) of local meteorological parameters,
18 including solar radiation, temperature (Temp), relative humidity (RH), wind direction
19 (WD) and wind speed (WS), and air quality parameters (i.e., NO_x, SO₂, O₃, PM₁) are
20 shown in Fig. S1. These parameters were provided by Guangdong Environmental
21 Monitoring Center (<http://www.gdemc.gov.cn/>). Ambient Temp, RH, and WS over the
22 study varied between 10.8–31 °C, 20.7–89.8%, and 0.2–3.9 m/s, with average values
23 of 21.2 °C, 59.9%, and 1.1 m/s, respectively. The concentration peaks for NO_x, SO₂,
24 and PM₁ were often observed during the nighttime, due to the accumulation of
25 pollutants under unfavorable meteorological conditions with lower WS and lower
26 boundary layer depth.

28 **2 The mass spectral patterns for the single particle types**

29 The mass spectral characteristics are displayed in Fig. S4, and a brief description
30 is provided as follows.

31 OC group: Mass spectra for OC particles mainly contain the OC markers, and also
32 some other OC peaks such as 50[C₄H₂]⁺, 51[C₄H₃]⁺, 55[C₄H₇]⁺ and 63[C₅H₃]⁺. Besides,
33 a large peak at m/z 39 is also observed in mass spectra of OC, which might be explained
34 by coagulation between OC and 39[K]⁺ or condensation of organic species onto
35 biomass seed [Moffet *et al.*, 2008]. Particle mass spectra in HMOC type show the
36 presence of m/z 50, 51, 63, 77, 91, 115, and 128 [Silva and Prather, 2000; Sodeman *et*

37 *al.*, 2005]. By including the ion peak from sulfate/nitrate, OC particles were subdivided
38 into OC-S, OC-SN, and HMOC.

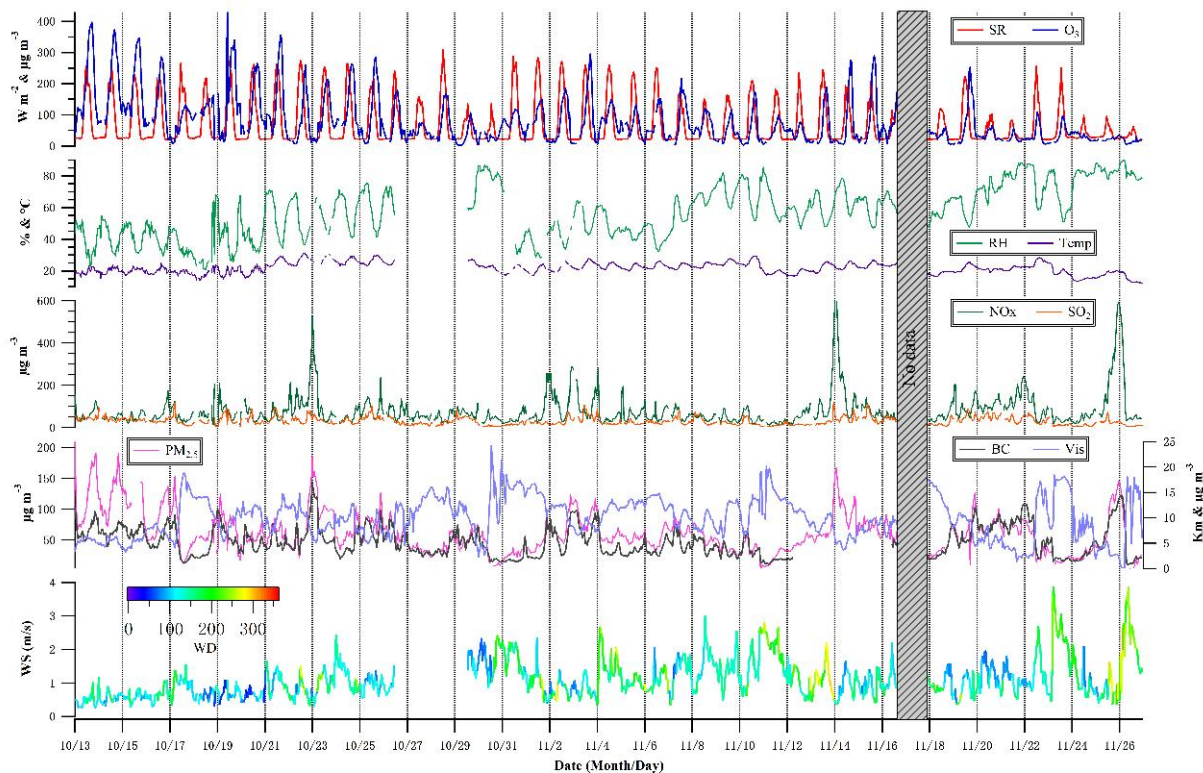
39 EC group: Mass spectra of LC-EC type are dominated by the distinct carbon ion
40 clusters ranged from m/z -120 to m/z 180, with minor ion intensities from other species.
41 SC-EC type is associated with short carbon clusters ions peaks ($C_n^{+/-}$, $n < 6$), generally
42 internally mixed with intense sulfate ion peak. Differently, NaK-EC type shows the
43 carbon ion clusters mainly in the negative mass spectra, combined with dominant peaks
44 from $23[Na]^+$ and $39[K]^+$ in the positive ones.

45 ECOC group: ECOC particles have typical carbon ion clusters ($12[C]^{+/-}$,
46 $24[C_2]^{+/-}$, ... , $12n[C_n]^{+/-}$) with $36[C_3]^+$ as dominant fragments, together with OC
47 markers (e.g., $27[C_2H_3]^+$, $29[C_2H_5]^+$, $37[C_3H]^+$, and $43[C_2H_3O]^+$). K-rich particles
48 contain potassium ($39[K]^+$), sulfate ($-97[HSO_4]^-$), nitrate ($-46[NO_2]^-$ and $-62[NO_3]^-$),
49 and carbonaceous species (e.g., $12[C]^+$, $27[C_2H_3]^+$, $29[C_2H_5]^+$, $36[C_3]^+$, $37[C_3H]^+$,
50 $43[C_2H_3O]^+$, $-26[CN]^-$, $-42[CNO]^-$) as major components, similar to those reported in
51 other studies [*Moffet et al.*, 2008; *Silva et al.*, 1999]. The association of sulfate and/or
52 nitrate separated the ECOC particles into ECOC-S, ECOC-SN, K-S, K-SN, and K-N
53 [*Zhang et al.*, 2015].

54 Metal rich group: Peaks corresponding to $23[Na]^+$, $39[K]^+$, $46[Na_2]^+$,
55 $81/83[Na_2Cl]^+$, nitrate and chloride ($-35[Cl]^-$ and $-37[Cl]^-$) are present in mass spectra
56 of Na-rich, indicating transport and evolution of sea salt particles [*Gaston et al.*, 2011;
57 *Gaston et al.*, 2013]. Na-K type is characterized by dominant peaks from $39[K]^+$,

58 relatively less intense peak from $23[\text{Na}]^+$, nitrate and silicate ($-76[\text{SiO}_3]^-$). They are
59 probably from dust and/or industry sources [*Moffet et al.*, 2008]. Fe-rich type is
60 identified by strong peaks from iron at m/z 54, 56 and 57, according to their isotopic
61 components. Similarly, Pb-rich type is identified by strong peaks m/z 206-208, and Cu-
62 rich is characterized by the presence of isotopic peaks at m/z 63 and 65. Fe-Cu-Pb
63 represents the internally mixed Fe, Cu, Pb in the individual particles.

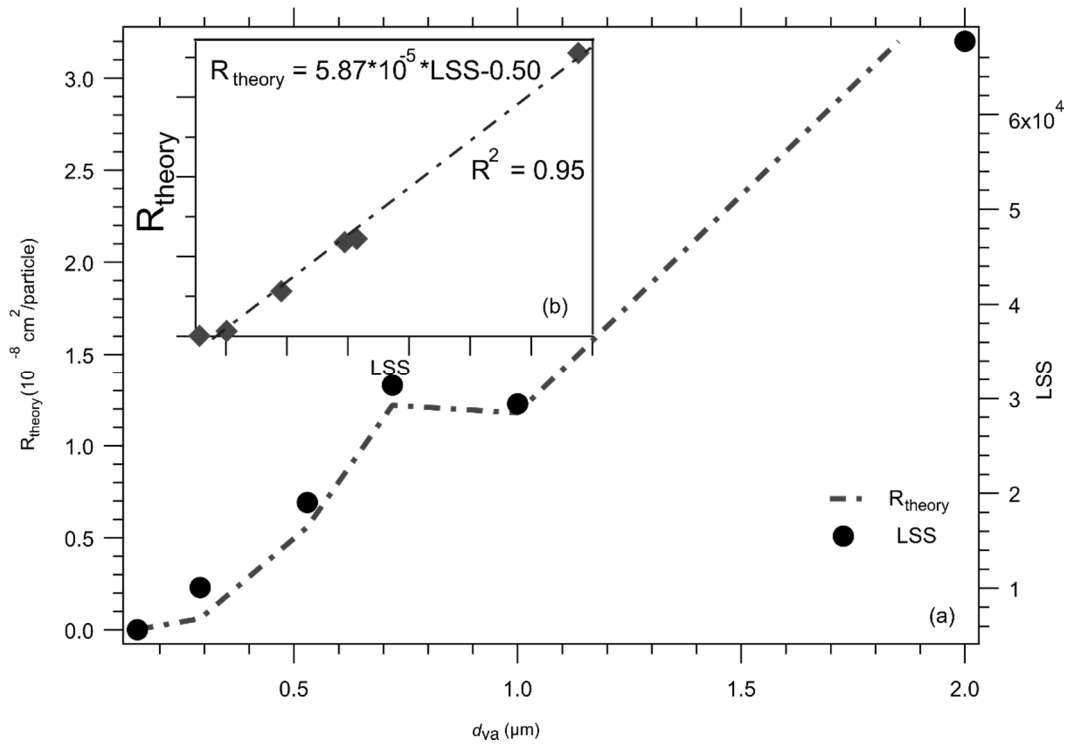
64



65

66

67 Fig. S1. Temporal profiles (in 1 h resolution) of PM₁, visibility, and black carbon (BC),
 68 gaseous pollutants (SO₂, NO_x, and O₃) and meteorological parameters, during the 13th
 69 October–26th November 2012 in Guangzhou.



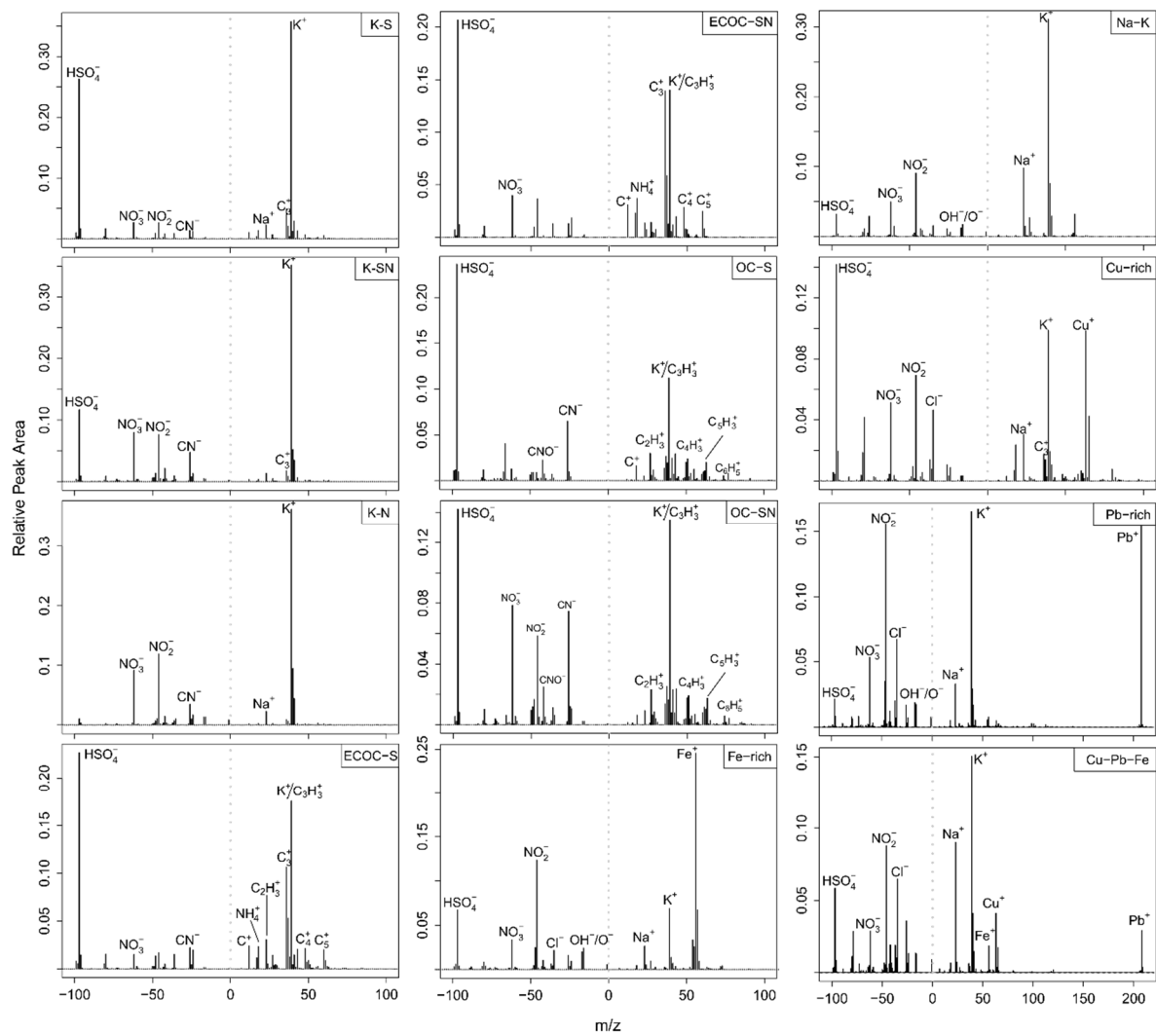
70

71

72 Fig. S2. (a) Upper limit of light scattering signals and theoretical PSCS for PSL as a

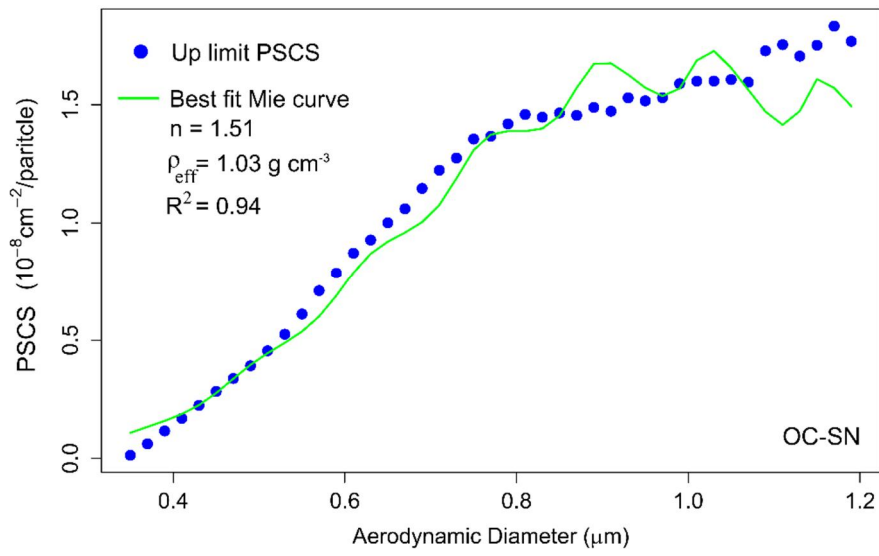
73 function of size (0.15, 0.3, 0.5, 0.72, 1, and 2 μm) and (b) their relationship. For PSL, $n = 1.59$

74 and $\rho_{\text{eff}} = \rho_p = 1.054 \text{ g cm}^{-3}$.



75

76 Fig. S3. Mass spectra for the observed single particle types in the atmosphere of Guangzhou
 77 during fall of 2012.

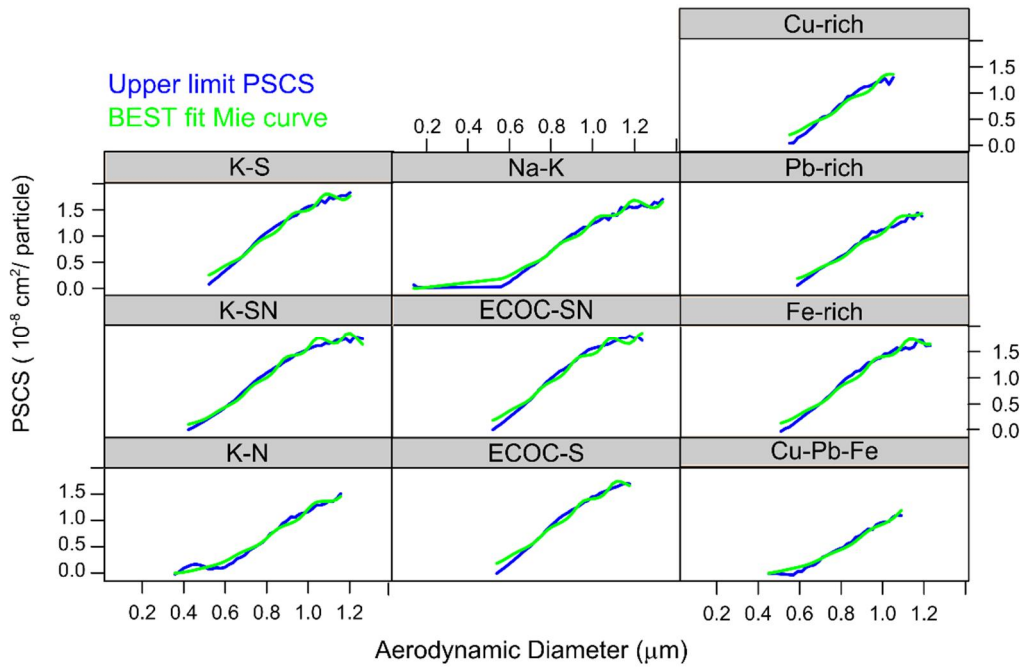


78

79

80

Fig. S4. Measured and best fit theoretical PSCS for OC-SN particle type.



81

82

83 Fig. S5. Measured and best fit theoretical PSCS for various particle types observed

84 in the present study.

85 **REFERENCES**

- 86 Gaston, C. J., H. Furutani, S. A. Guazzotti, K. R. Coffee, T. S. Bates, P. K. Quinn, L. I.
87 Aluwihare, B. G. Mitchell, and K. A. Prather (2011), Unique ocean-derived particles
88 serve as a proxy for changes in ocean chemistry, *J. Geophys. Res.-Atmos.*, *116*(D18310),
89 1-13, doi:10.1029/2010jd015289.
- 90 Gaston, C. J., P. K. Quinn, T. S. Bates, J. B. Gilman, D. M. Bon, W. C. Kuster, and K. A.
91 Prather (2013), The impact of shipping, agricultural, and urban emissions on single
92 particle chemistry observed aboard the R/V Atlantis during CalNex, *J. Geophys. Res.-*
93 *Atmos.*, *118*(10), 5003-5017, doi:10.1002/Jgrd.50427.
- 94 Moffet, R. C., B. de Foy, L. T. Molina, M. J. Molina, and K. A. Prather (2008), Measurement
95 of ambient aerosols in northern Mexico City by single particle mass spectrometry,
96 *Atmos. Chem. Phys.*, *8*(16), 4499-4516.
- 97 Silva, P. J., D. Y. Liu, C. A. Noble, and K. A. Prather (1999), Size and chemical
98 characterization of individual particles resulting from biomass burning of local Southern
99 California species, *Environ. Sci. Technol.*, *33*(18), 3068-3076.
- 100 Silva, P. J., and K. A. Prather (2000), Interpretation of mass spectra from organic compounds
101 in aerosol time-of-flight mass spectrometry, *Anal. Chem.*, *72*(15), 3553-3562.
- 102 Sodeman, D. A., S. M. Toner, and K. A. Prather (2005), Determination of single particle
103 mass spectral signatures from light-duty vehicle emissions, *Environ. Sci. Technol.*,
104 *39*(12), 4569-4580.
- 105 Song, X. H., P. K. Hopke, D. P. Fergenson, and K. A. Prather (1999), Classification of single
106 particles analyzed by ATOFMS using an artificial neural network, ART-2A, *Anal.*
107 *Chem.*, *71*(4), 860-865.
- 108 Zhang, G. H., B. X. Han, X. H. Bi, S. H. Dai, W. Huang, D. H. Chen, X. M. Wang, G. Y.
109 Sheng, J. M. Fu, and Z. Zhou (2015), Characteristics of individual particles in the
110 atmosphere of Guangzhou by single particle mass spectrometry, *Atmos. Res.*, *153*(0),
111 286-295, doi:10.1016/j.atmosres.2014.08.016.